JOURNAL OF RAMAN SPECTROSCOPY
J. Raman Spectrosc. 2008; **39**: 1338–1342
Published online 18 April 2008 in Wiley InterScience
(www.interscience.wiley.com) DOI: 10.1002/jrs.1999

JRS

Plasmon-enhanced polarized Raman spectroscopy for sensitive surface characterization

J. Kasim,[1,3] X. Y. Tee,[1] Y. M. You,[1] Z. H. Ni,[1] Y. Setiawan,[2,3] P. S. Lee,[2] L. Chan[3] and Z. X. Shen[1]*

[1] Division of Physics and Applied Physics, School of Physical and Mathematical Sciences, Nanyang Technological University, Singapore 637616, Singapore
[2] School of Materials Science and Engineering, Nanyang Technological University, Singapore 639798, Singapore
[3] Chartered Semiconductor Manufacturing Ltd, Singapore 738406, Singapore

Received 12 December 2007; Accepted 11 March 2008

Local-mode and localized surface plasmons generated on the silver thin film can selectively enhance the Raman signal from the surface. Further improvement of surface signal can be obtained by using the polarized Raman technique that results in a dramatic enhancement of the surface sensitivity by up to 25.4 times as compared to that without a silver coating. This technique will be very useful for Raman study on samples that suffer overlapping background signal. In this article, we show that it can be used to significantly improve the signal of thin strained-Si layer on top of SiGe buffer layer. Copyright © 2008 John Wiley & Sons, Ltd.

KEYWORDS: Raman spectroscopy; surface plasmons; strained-Si; depolarization; enhancement

INTRODUCTION

Surface-enhanced Raman spectroscopy (SERS) has been a successful and powerful method for sensitive Raman detection of low concentrations of simple organic and complex biological molecules.[1,2] It has been successfully used to detect low molecule concentration that cannot be detected by normal Raman spectroscopy.[3,4] However, this technique cannot be applied to thin film on a substrate, e.g. the strain study on thin strained-Si film on SiGe substrate, which is one of the most important methods used to improve the microchips' performance.[5–7] Tensile strained-Si can be utilized by using the $Si_{1-x}Ge_x$ as a buffer layer for n-MOSFET application, while compressively strained-Si is achieved by using $Si_{1-y}C_y$ buffer layer for p-MOSFET.[8] In strained-Si, the intervalley scattering will be suppressed and the effective carrier mass will be reduced, hence resulting in an improvement of the effective carrier mobility in the Si channel. This phenomenon enables us to achieve a higher transistor performance by a few times without changing its physical size.[9,10] Since mobility enhancement in the strained-Si depends on the amount of strain that is applied to the channel region,[11] accurate strain determination is extremely important.

*Correspondence to: Z. X. Shen, Division of Physics and Applied Physics, School of Physical and Mathematical Sciences, Nanyang Technological University, Singapore 637616, Singapore.
E-mail: zexiang@ntu.edu.sg

Techniques such as converging beam electron diffraction (CBED) in transmission electron microscopy (TEM)[12,13] and X-ray diffraction (XRD)[14,15] have been used to study the strain in materials. Although the former technique has a high spatial resolution, the sample preparation is very complicated. For the latter technique, localized strain determination will be difficult since the X-rays cannot be focused into a small spot easily and will penetrate deep into the silicon sample. On the other hand, Raman spectroscopy has been a versatile technique in strain determination.[16–18] The Raman peak shift is sensitive to strain and can be used for quantitative strain determination.[19,20] However, due to the large penetration depth of the laser into silicon (about 1 μm for 532 nm laser),[21] a problem arises when Raman spectroscopy is employed to measure the strain in a very thin strained-Si layer grown on a SiGe buffer layer. Since the Si–Si Raman peak from the buffer layer is very strong and the peak position is close to the Si–Si Raman peak position from the strained-Si, the strain determination of strained-Si layer becomes very complicated and less accurate.

To solve this problem, Hayazawa *et al*.[22] enhanced the signal from the thin strained-Si layer (30 nm) by coating 10 nm silver thin film on top of the sample. Unlike the conventional surface-enhanced Raman spectroscopy (SERS) experiments where the molecular sample is deposited on top of roughened metal surface or metallic nanoparticles,[23–25] the strained-Si sample is coated with a thin metal layer instead.

The enhancement of the surface Raman signal is due to the generation of local-mode plasmons, which is due to the collective oscillation of electrons at small metallic particle with the incident light.

Apart from the local-mode plasmons, propagating surface plasmons that are excited by a large numerical aperture (NA) objective lens can interfere with each other to produce a strong localized electromagnetic field in the focus region.[26,27] This is the localized surface plasmons, which is the collective oscillation of electrons on a 'flat' metal surface by a focused beam.[28]

In this article, we show the improvement of the Raman signal by both the local-mode plasmons and the localized surface plasmons from silver thin film on a 20 nm strained-Si layer grown on a SiGe buffer layer. We also carried out polarization Raman study. We show that using an analyzer at cross polarization with the laser polarization, the Raman signal from the SiGe buffer layer can be reduced and the surface sensitivity can be enhanced further, allowing more accurate strain determination of the thin strained-Si layer.

EXPERIMENTAL

The Raman spectra were recorded using a WITec CRM200 confocal Raman microscopy system with an Olympus microscope objective lens (60 × NA = 1.2 water immersion). The excitation source was a 532-nm laser (2.33 eV), which was coupled into the system using a single-mode fiber. Raman signals from the (001) face of the samples were collected by the lens in the backscattered configuration without analyzer $[z(x, xy)\bar{z}]$ or with rotating analyzer axes with respect to laser polarization $\{z[x, xy(\theta)]\bar{z}\}$ to a 1800 lines/mm grating and detected by a TE-cooled charge-coupled device (CCD), as shown in Fig. 1(a). The inset of Fig. 2 shows the schematic diagram illustrating the cross-sectional view of the sample. The sample consists of 20 nm strained-Si layer grown on 1 μm relaxed $Si_{0.75}Ge_{0.25}$/2 μm graded $Si_{1-x}Ge_x$ ($x = 0$ to 0.25)/bulk silicon. Silver thin films with different thicknesses (5, 10, 15 and 20 nm) were deposited on the samples using DC magnetron sputtering in vacuum. Silver was used because it is the most effective surface-enhanced medium for SERS among all metals in the visible region.[29,30] During the experiments, a 150 μm thick cover glass ($n_r = 1.45$) was pressed onto the samples, leaving a small air gap between the cover glass and the silver film. In the later experiments, the effect of adding an analyzer was studied. An analyzer was placed after the edge filter, as shown in Fig. 1(a).

RESULTS AND DISCUSSION

Figure 2 shows the Raman spectra from uncoated and silver-coated samples. There are two peaks in the spectra, located at 502 and 511.8 cm^{-1}, respectively. The first peak is the Si–Si peak from the relaxed SiGe layer, which is underneath the strained-Si layer. The second peak is the Si–Si peak

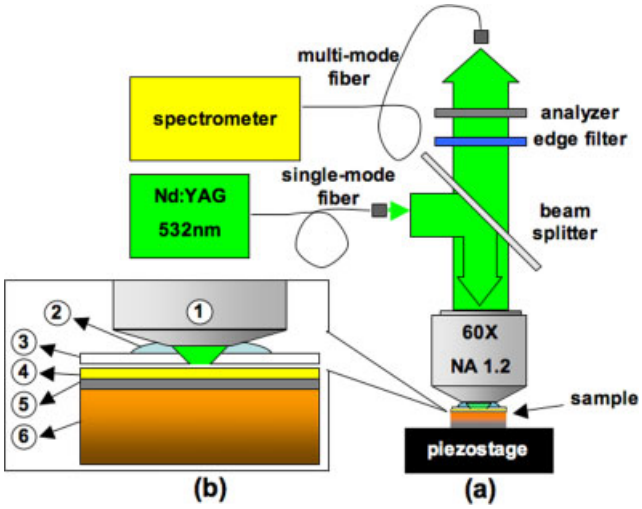

Figure 1. (a) Schematic diagram of the experimental setup. (b) Zoom-in view of the objective lens and the sample. Water immersion objective lens (1) that is immersed in water (2) is used to focus the excitation laser to the sample. Points (3)–(6) correspond to the cover glass, the silver coating; the strained-Si layer and the substrate, respectively. This figure is available in colour online at www.interscience.wiley.com/journal/jrs.

from the strained-Si layer. This peak is used to determine the strain value as the phonon frequency is related to the lattice constant, hence the strain. However, the intensity of the strained-Si peak is much weaker than that from the SiGe layer because the strained-Si layer is much thinner compared to the SiGe layer, making strain determination using the strained-Si peak position very difficult. This is particularly true for samples with a smaller Ge concentration in the SiGe layer where the Raman peaks due to strained-Si and SiGe overlap much more severely.

Surface-enhanced Raman spectroscopy by silver coating was then used to enhance the signal from strained-Si. The local-mode plasmons can be excited by the natural roughness of the silver film, however, in order to excite the localized surface plasmons, the component of the incident laser wave vector parallel to the metal surface, $k_{parallel}$, has to be equal to the wave vector of the surface plasmons (k_{sp}). This is to satisfy the conservation of energy and momentum.

$$\omega_{sp}^2 = \frac{\omega_p^2}{2} + (ck)^2 - [\frac{\omega_p^4}{4} + (ck)^4]^{1/2} \quad (1)$$

$$\omega_p = \frac{ne^2}{m_e \varepsilon_0} \quad (2)$$

The dispersion relation for surface plasmons will not intersect with the dispersion curve for light in air, $\omega = ck$, as shown in Eqn (1),[31] where ω_p is the bulk plasma frequency of metal; n is number of conduction electrons; e is the charge of electron; m_e is the effective mass of electron; and ε_o is the permittivity in vacuum. This is because k_{sp}

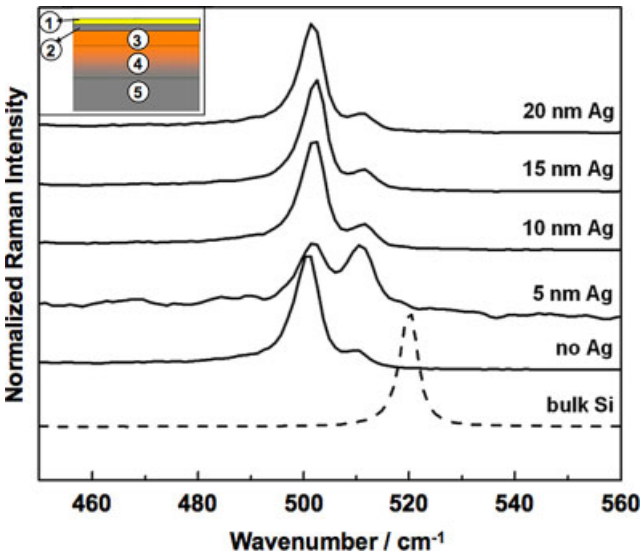

Figure 2. Raman spectra of strained-Si sample coated with different thickness of silver. The Raman peak at ~502 cm^{-1} belongs to the SiGe layer while that at ~512 cm^{-1} belongs to strained-Si. The dashed spectrum shows the Raman spectrum from the bulk silicon for comparison. The spectra have been shifted vertically for clarity. It is clear that the relative peak intensity for the strained-Si peak is strongest for the 5 nm Ag coated sample. Inset shows the schematic diagram illustrating the cross-sectional view of the sample (not to scale). Points (1)–(5) correspond to the silver coating, the strained-Si layer, the relaxed $Si_{0.75}Ge_{0.25}$ layer, the graded $Si_{1-x}Ge_x$ ($x = 0$–0.25) layer and the bulk silicon, respectively. This figure is available in colour online at www.interscience.wiley.com/journal/jrs.

of the surface plasmons is larger than $k_{parallel}$ of incident light in air; hence the conservation of momentum cannot be satisfied. Therefore, surface plasmons cannot be excited in this manner. In order to couple photons into surface plasmons, it is necessary to increase the momentum of the incident light. This can be achieved by passing the light through a medium that has higher refractive index (n_r) than air, e.g. the cover glass, and bring it near the metal surface. Hence, surface plasmons can be excited when $k_{parallel}$ of the evanescent wave, which is present in total internal reflection, can match the k_{sp} at a certain incident angle α, as shown in Eqn (3).[32]

$$k_{sp} = k_{parallel} = \frac{\omega}{c} n_r \sin\alpha \tag{3}$$

In our study, a large NA objective lens (NA = 1.2) was used to satisfy the dispersion-matching condition between light and the surface plasmons. The surface plasmon field will oscillate perpendicularly and propagate parallel to the metal surface in many directions. As discussed earlier, at the focus region the surface plasmons will interfere with each other to form strong localized electric field, i.e. localized surface plasmons. The Raman signals induced by the plasmons are depolarized from the polarization of laser.[33] This depolarization effect is exploited in our study to increase the relative Raman peak intensity of the strained-Si layer using polarized Raman spectroscopy later on.

The Raman spectra of samples after silver coating are shown in Fig. 2. We observed that the intensity of the Si–Si peak from strained-Si increased after silver coating. Throughout this work, surface enhancement is defined as follows:

$$Surface\_enhancement = \frac{r_{silver-coated}}{r_{uncoated}} \tag{4}$$

$$r = \frac{I_{strained-Si}}{I_{SiGe}} \tag{5}$$

where I is the intensity of the Raman signal in the corresponding layer. The optimum silver thickness was about 5 nm for the highest surface enhancement, which is 12.89 times enhanced as compared to that of the uncoated sample. As the thickness of the silver film increases, the enhancement will decrease. This is due to the exponential decay of the surface plasmons into the silver film. As a comparison, surface enhancement of 5.23 times was obtained when cover glass was not used (in this case dry objective lens was used, NA = 0.95). The enhancement of 12.89 can be attributed to the contributions from the localized surface plasmons and the local-mode plasmons, while the enhancement of 5.23 can be attributed to the contribution from the local-mode plasmons alone. This further demonstrates the existence of localized surface plasmons and the role of the cover glass in exciting it, as shown in Eqn (3).

To further increase the relative Raman signal of the strained-Si layer, we used the fact that the polarization of the surface-enhanced Raman signal is different from that of the normal signal. Several groups have also taken advantage of the polarization dependence of the sample to improve the sensitivity for Raman enhanced experiments.[34–36] By using different analyzer angles, we can choose the signal from different polarizations. The angle θ here represents the angle between the analyzer axis and the laser polarization, as shown in the inset of Fig. 3(a). Figure 3(a) shows the Raman spectra at different analyzer angles. Figure 3(b) shows the Raman intensities of SiGe and strained-Si layers at different analyzer angles. As analyzer angle increases, both SiGe and strained-Si signals decrease. However, it can be observed that the strained-Si signal decreases at a slower rate than that of SiGe. Figure 3(c) shows the ratio of strained-Si over SiGe signals from uncoated and coated samples as a function of analyzer angle. For the uncoated sample, the ratio does not change with the analyzer angle. This is because both Raman signals from strained-Si and SiGe are polarized to the laser polarization. By coating a thin layer of silver, surface plasmons are excited by the incident laser. While the incoming laser is polarized, the surface plasmons can cause

DOI: 10.1002/jrs

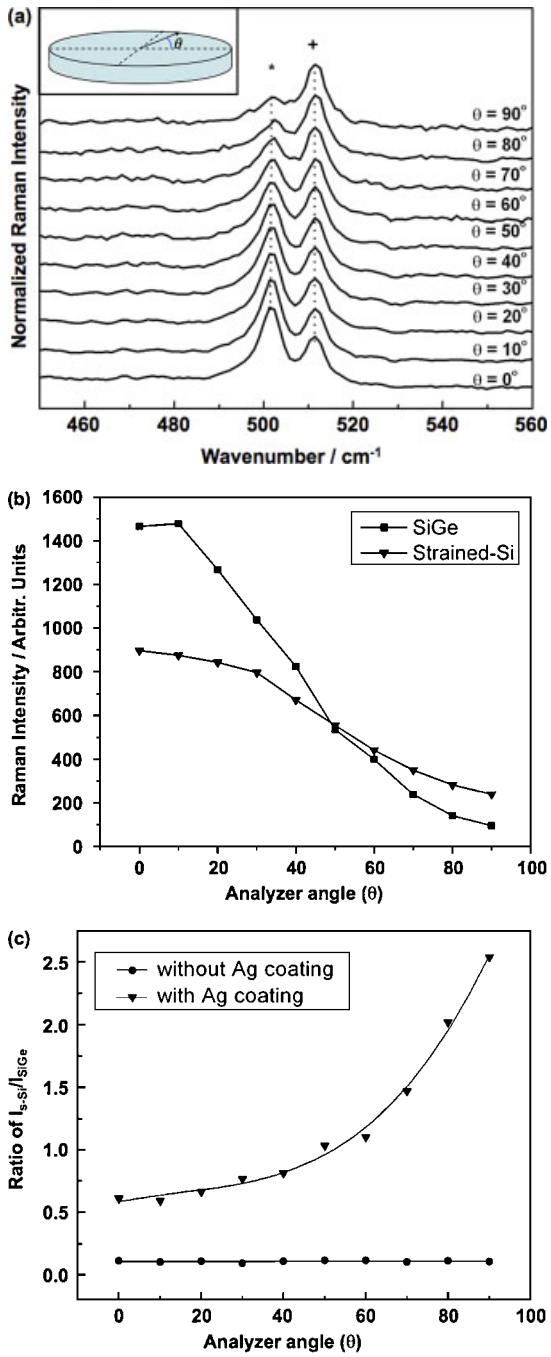

Figure 3. (a) Raman spectra of 5 nm silver coating at different analyzer angles with respect to the laser polarization. All the spectra have been shifted vertically for clarity; (*) and (+) show the Si–Si LO phonon mode from the relaxed SiGe and strained silicon layers, respectively. (b) Raman intensities of SiGe and strained-Si at different analyzer angles. (c) The ratio of strained-Si and SiGe signals for uncoated and 5 nm silver-coated sample at different analyzer angles, respectively. Inset in Fig. 3(a) shows the schematic diagram of the analyzer. $\theta = 0°$ represents the analyzer axis parallel to the laser polarization. This figure is available in colour online at www.interscience.wiley.com/journal/jrs.

enhanced depolarized Raman scattering from the sample, as discussed earlier. So, as the analyzer angle was rotated from 0° to 90° in consecutive steps of 10° with respect to the polarization of laser, which is linearly polarized at 0°, the ratio of strained-Si and SiGe signals increased. It reached the maximum when the angle was at 90°. The role of the analyzer here is to remove the Raman signals that are not enhanced by the surface plasmons (far-field signal). At 90°, the analyzer will remove the far-field signals, and the enhanced Raman signals due to surface plasmons, which are depolarized, will still be detected. With this approach, surface enhancement of 25.4 times can be obtained. It can also be observed from Fig. 3(a) and (b) that even when the analyzer is at 90° the intensity of SiGe is not completely removed. This is because the plasmon propagation length is more than the thickness of the strained silicon. Hence the SiGe signal near the strained silicon layer can still be enhanced by the surface plasmons, but it is much weaker.

CONCLUSION

In conclusion, we have shown that combination of local-mode plasmons and localized surface plasmons on thin metal surface can be used to enhance the surface sensitivity of Raman spectroscopy. This approach is very useful when the Raman signal from the surface is obscured by the signal beneath, for example, in strained-Si grown on a SiGe layer. In our study, the optimum silver thickness for the best enhancement is 5 nm. An analyzer can be used to remove the far-field signal when it is at 90° to the polarization of laser. The near-field enhanced Raman signal that is depolarized can be detected, and surface enhancement up to 25.4 times can be achieved.

Acknowledgements

The authors would like to acknowledge Nanyang Technological University and Chartered Semiconductor Manufacturing for the financial support.

REFERENCES

1. Michaels AM, Nirmal M, Brus LE. *J. Am. Chem. Soc.* 1999; **121**: 9932.
2. Etchegoin P, Liem H, Maher RC, Cohen LF, Brown RJC, Milton MJT, Gallop JC. *Chem. Phys. Lett.* 2003; **375**: 84.
3. Lee SJ, Morrill AR, Moskovits M. *J. Am. Chem. Soc.* 2006; **128**: 2200.
4. Becker M, Sivakov V, Andra G, Geiger R, Schreiber J, Hoffmann S, Michler J, Milenin AP, Werner P, Christiansen SH. *Nano Lett.* 2007; **7**: 75.
5. Rosenberg R, Edelstein DC, Hu CK, Rodbell KP. *Annu. Rev. Mater. Sci.* 2000; **30**: 229.
6. Lee ML, Fitzgerald EA, Bulsara MT, Currie MT, Lochtefeld A. *J. Appl. Phys.* 2005; **97**: 011101.
7. Schaffler F. *Semicond. Sci. Technol.* 1997; **12**: 1515.
8. Ang KW, Lin JQ, Tung CH, Balasubramanian N, Samudra G, Yeo YC. *Symposium on VLSI Technology Digest of Tehnical Papers*, Kyoto, Japan. 2007; 42 .
9. Schaffler F. *Thin Solid Films* 1998; **321**: 1.

10. Vartanian V, Zollner S, Thean AVY, White T, Nguyen BY, Prabhu L, Eades D, Parsons S, Desjardins H, Kim K, Jiang ZX, Dhandapani V, Hildreth J, Powers R, Spencer G, Ramani N, Kottke M, Canonico M, Wang XD, Contreras L, Theodore D, Gregory R, Venkatesan S. *IEEE Trans. Semicond. Manuf.* 2006; **19**: 381.
11. Paul DJ. *Semicond. Sci. Technol.* 2004; **19**: R75.
12. Senez V, Artigliato A, Wolf ID, Carnevale G, Balboni R, Frabboni S, Benedetti A. *J. Appl. Phys.* 2003; **94**: 5574.
13. Liu HH, Duan XF, Qi XY, Xu QX, Li HO, Qian H. *Appl. Phys. Lett.* 2006; **88**: 263513.
14. Vinci RP, Vlassak JJ. *Annu. Rev. Mater. Sci.* 1996; **26**: 431.
15. Erdtmann M, Langdo TA. *J. Mater. Sci.: Mater. Electron.* 2006; **17**: 137.
16. Wolf ID, Maes HE, Jones SK. *J. Appl. Phys.* 1996; **79**: 7148.
17. Nakashima S, Yamamoto T, Ogura A, Uejima K, Yamamoto T. *Appl. Phys. Lett.* 2004; **84**: 2533.
18. Mitani T, Nakashima S, Okumura H, Ogura A. *J. Appl. Phys.* 2006; **100**: 073511.
19. Anastassakis E, Liarokapis E. *J. Appl. Phys.* 1987; **62**: 3346.
20. Anastassakis E, Cantarero A, Cardona M. *Phys. Rev. B* 1990; **41**: 7529.
21. Wolf ID. *Semicond. Sci. Technol.* 1996; **11**: 139.
22. Hayazawa N, Motohashi M, Saito Y, Kawata S. *Appl. Phys. Lett.* 2005; **86**: 263114.
23. Freeman RG, Grabar KC, Allison KJ, Bright RM, Davis JA, Guthrie AP, Hommer MB, Jackson MA, Smith PC, Walter DG, Natan MJ. *Science* 1995; **267**: 1629.
24. Nie SM, Emory SR. *Science* 1997; **275**: 1102.
25. Kneipp K, Wang Y, Kneipp H, Perelman LT, Itzkan I, Dasari R, Feld MS. *Phys. Rev. Lett.* 1997; **78**: 1667.
26. Kano H, Mizuguchi S, Kawata S. *J. Opt. Soc. Am. B* 1998; **15**: 1381.
27. Kano H, Knoll W. *Opt. Commun.* 1998; **153**: 235.
28. Kano H, Knoll W. *Opt. Commun.* 2000; **182**: 11.
29. Cao YWC, Jin RC, Mirkin CA. *Science* 2002; **297**: 1536.
30. Dieringer JA, McFarland AD, Shah NC, Stuart DA, Whitney AV, Yonzon CR, Young MA, Zhang XY, Van Duyne RP. *Faraday Discuss.* 2006; **132**: 9.
31. Pitarke JM, Silkin VM, Chulkov EV, Echenique PM. *Rep. Prog. Phys.* 2007; **70**: 1.
32. Otto A. *Z. Phys.* 1968; **216**: 398.
33. Isfort G, Schierbaum K, Zerulla D. *Phys. Rev. B* 2006; **74**: 033404.
34. Ossikovki R, Nguyen Q, Picardi G. *Phys. Rev. B* 2007; **75**: 045412.
35. Lee N, Hartschuh RD, Mehtani D, Kisliuk A, Maguire JF, Green M, Foster MD, Sokolov AP. *J. Raman Spectrosc.* 2007; **38**: 789.
36. Hayazawa N, Motohashi M, Saito Y, Ishitobi H, Ono A, Ichimura T, Verma P, Kawata S. *J. Raman Spectrosc.* 2007; **38**: 684.

DOI: 10.1002/jrs